

# State-specific lifetime determination of the $a^3\Pi$ state in CO

Rienk T. Jongma,<sup>a)</sup> Giel Berden, and Gerard Meijer<sup>b)</sup>

*Department of Molecular and Laser Physics, University of Nijmegen Toernooiveld, 6525 ED Nijmegen, The Netherlands*

(Received 19 June 1997; accepted 4 August 1997)

Two different techniques were applied to measure the lifetime of the lowest rotational levels in the metastable  $a^3\Pi_1(v=0)$  state of CO. First, measurement of the absolute absorption cross-section for several absorption lines of the  $a(v=0)\leftarrow X(v=0)$  transition yields an Einstein coefficient of  $A_{0,0}=97\pm 3\text{ s}^{-1}$ . In combination with the experimentally determined branching ratios for the  $a\rightarrow X$  transition, the lifetime of each component of the  $a^3\Pi_1(v=0, J=1)$   $\Lambda$ -doublet is determined to be  $3.67\pm 0.20\text{ ms}$ . Second, detection of the spin-forbidden fluorescence at two positions in the molecular beam downstream from the excitation region, as a function of velocity of the molecules directly probes the exponential decay. With this technique the lifetime of the lower component of the same  $a^3\Pi_1(v=0, J=1)$   $\Lambda$ -doublet is determined to be  $3.4\pm 0.4\text{ ms}$ , while for the upper component a value of  $3.8\pm 0.5\text{ ms}$  is found. © 1997 American Institute of Physics. [S0021-9606(97)00942-2]

## I. INTRODUCTION

The determination of the radiative lifetime of metastable states in molecules is in general not straightforward. Conventional gas phase techniques measure the decay time of the fluorescence signal in a molecular beam or in a cell, but these techniques are only applicable for radiative lifetimes up to several microseconds. For the determination of the radiative lifetime of metastable states there are some extra difficulties. First, the preparation of single quantum levels in the excited state using direct laser excitation is difficult because the transition to the excited state is very weak, inherent to being a metastable state. Second, molecules with long lived excited states may escape from the detection region. And third, the population can be redistributed over other levels due to quenching during their lifetime; even small quenching rates will have a significant influence on the observed lifetime.

Here we report on two different types of experiments to determine the radiative lifetime of single rotational levels of the metastable  $a^3\Pi$  state in CO. In the early 1970s calculations and many experiments have been performed to determine the lifetime of the metastable  $a^3\Pi$  state of CO. The interest in metastable CO molecules was triggered by the presence of strong features of the Cameron bands of CO in the emission spectrum of Mars. James calculated the oscillator strength to, and the corresponding lifetime of, the  $a^3\Pi(v=0)$  state assuming spin-orbit coupling to the  $A^1\Pi$  state.<sup>1</sup> The spin-forbidden  $a^3\Pi\leftarrow X^1\Sigma^+$  transition, thereby borrows intensity from the  $A^1\Pi\leftarrow X^1\Sigma^+$  transition due to the amount of  $^1\Pi$  character in the  $^3\Pi$  wavefunction. The oscillator strength was found to be  $f_{0,0}=1.63\times 10^{-7}$ , corresponding to an averaged electronic lifetime (assuming an equal distribution of intensity over each  $\Lambda$ -doublet component in each  $\Omega$ -ladder) of  $\tau_{av}=8.75\text{ ms}$ . The transition

strength to, and thereby the radiative lifetime of a certain rotational level in the  $a^3\Pi$  state is determined by the fraction of singlet character in the wavefunction, and is strongly dependent on the quantum numbers  $J$  and  $\Omega$ .<sup>1</sup>

Various experiments from that same period that claim a high degree of accuracy give oscillator strengths that correspond to averaged lifetimes between 1 and 9.4 ms.<sup>2-7</sup> This averaged lifetime is normally obtained from cell experiments, where generally a large number of rotational levels is populated in the upper state, and pressures are such that collisional redistribution occurs within the lifetime of the excited state.

Up to this moment, however, no experiments are reported in which precise values for the radiative lifetime of single rotational levels in the  $a^3\Pi$  state of CO are determined. For the interpretation of experiments involving metastable CO, like surface scattering experiments with state-selected CO ( $a^3\Pi$ ) molecules<sup>8,9</sup> or photodissociation experiments monitoring CO neutral time-of-flight,<sup>10,11</sup> not the knowledge of the averaged lifetime but accurate knowledge of the lifetime of single quantum levels in the  $a^3\Pi(v=0)$  state is required.

A straightforward way to detect metastable CO molecules in a molecular beam is via detection of their spontaneous fluorescence.<sup>12</sup> Although the  $a\rightarrow X$  electric dipole transition is very weak, all molecules will eventually decay back to the electronic ground state via emission of photons in the absence of other deactivation mechanisms. The detection efficiency of this laser induced fluorescence (LIF) signal depends on the solid angle and the detection volume that can be monitored, as well as on the time that the metastable CO molecules spend in the detection region, i.e., on their velocity. It is possible to obtain a complete separation in time of fluorescence of the long lived metastable CO molecules and straylight caused by the laser, and by probing a large detection volume, fluorescence measurements lead to sensitive detection of the electronically excited CO molecules. The experiments reported here all make use of the detection of this

<sup>a)</sup>Present address: Department of Chemistry, University of California, Santa Barbara, CA 93106.

<sup>b)</sup>Author to whom correspondence should be addressed; Electronic mail: gerardm@sci.kun.nl

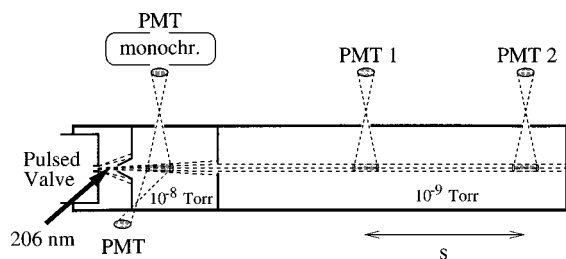


FIG. 1. Schematic representation of the molecular beam machine. A valve releases gas pulses of a mixture of 20% CO in a rare gas. After excitation to the metastable  $a^3\Pi$  state in the source chamber, the molecular beam is collimated by a 0.8 mm diam skimmer. In the first detection area, located 7.5 cm downstream from the excitation region, the spin-forbidden  $a \rightarrow X$  fluorescence can be monitored both in horizontal (total fluorescence) and vertical (dispersed fluorescence) direction. For the two-point lifetime measurements the fluorescence is monitored in vertical direction by PMTs mounted 1 and 1.8 m downstream from the excitation region. To obtain a well-collimated molecular beam with a low divergence, a second 1.2 mm diam skimmer is mounted 0.5 m downstream from the excitation region.

spin-forbidden fluorescence of the metastable CO molecules.

Direct absorption measurements provide a general applicable technique to measure lifetimes and are also applicable to measure the lifetime of long lived excited states. For this it is needed that all decay and relaxation channels from the excited state are known. In practice, this means that all possible relaxation channels to dark and dissociative states and radiative relaxation channels must be known.

To obtain the lifetime of the  $a^3\Pi$  state of CO, first the branching ratios of the  $a(v=0) \rightarrow X(v'')$  emission, previously calculated by James,<sup>1</sup> are determined experimentally by dispersing the fluorescence of metastable CO molecules in a molecular beam. Second, the absolute peak absorption cross-section of CO is measured in an almost 2-m-long, room temperature absorption cell. The combination of absorption and dispersion measurements puts the value of the branching ratios on an absolute scale and allows determination of the radiative lifetime of the  $a^3\Pi$  state. For the direct absorption measurements, a molecular beam machine is applied as a narrow-band detection system ( $\approx 200$  MHz) to circumvent problems related to the spectral profile of the laser.

An alternative approach to measure the lifetime of the  $a^3\Pi$  state of CO is the detection of the spin-forbidden  $a \rightarrow X$  fluorescence at two different positions in the molecular beam, downstream from the excitation region. By varying the velocity of the CO molecules in the molecular beam, i.e., by varying the time-delay between both fluorescence signals, the exponential decay of the population in the  $a^3\Pi$  state is directly probed.

## II. DISPERSION AND ABSORPTION MEASUREMENTS

### A. Experiment

The vacuum machine in which the measurements are performed is schematically indicated in Fig. 1 and has been discussed in detail before.<sup>12,13</sup> A pulsed molecular beam machine, consisting of two differentially pumped vacuum

chambers, is connected to an ultrahigh vacuum (UHV) system. At the end of the UHV system, a 1-m-long flight tube is mounted to increase the flight distance that the molecules can travel. Three different fluorescence detection regions are present at 7.5 cm, 1 and 1.8 m downstream from the excitation region. For the dispersion and absorption measurements, only the first detection region is used.

The pulsed molecular beam is produced by expanding a gas mixture of 20% CO seeded in He, Ne, Ar, Kr, or Xe. The metastable CO molecules are produced in the source chamber, before the molecular beam is skimmed.

In these experiments a pulsed dye amplified (PDA) laser system (Lambda Physik LPD3000), pumped by a Nd:YAG laser (Spectra Physics GCR-190 without injection-seeder), is used to excite the ground state CO molecules. The seeding of the PDA-system is performed with a single-mode *cw* ring dye laser system (Spectra Physics 380), pumped by an Ar-ion laser (Spectra Physics 2017). The output of the PDA-system (around 618 nm) is frequency tripled in the combination of a potassium dihydrogen phosphate (KDP) and a  $\beta$ -BaB<sub>2</sub>O<sub>4</sub> (BBO) crystal, providing 0.5 mJ/pulse of 206 nm laser radiation in a bandwidth of 150 MHz full width at half-maximum (FWHM).

The spectral profile of this laser shows a 150-MHz-wide laser peak, superimposed on a spectrally broad background.<sup>14</sup> The integrated intensity of the broad background is even larger than the integrated intensity of the narrow-band laser peak. This spectral profile directly reflects the time-profile of the pulse delivered by the nonseeded Nd:YAG laser that is used to pump the PDA system.

For the dispersed fluorescence measurements the PDA system is used to excite the CO molecules 2 cm downstream from the nozzle before they pass through a 0.8 mm diam skimmer. After the skimmer, in the second differentially pumped vacuum chamber, the spin-forbidden fluorescence of the metastable CO molecules back to the electronic ground state is detected in the first fluorescence detection region perpendicularly to the molecular beam axis, both in horizontal and vertical direction, at a distance of 7.5 cm downstream from the excitation region.

The nondispersed fluorescence that is emitted in horizontal direction is detected with a photomultiplier (PMT) and is used as a calibration signal to correct for fluctuations. The fluorescence in vertical direction is collected by a lens, imaged on the entrance slit of the monochromator (Oriel 77250; resolution set to  $\sim 3$  nm in the 200–300 nm region), and detected with a second PMT. The PMT-signals are digitized and displayed on an oscilloscope with a 100 MHz sampling rate and a 10 bit vertical resolution (Lecroy 9430), which can be read out by PC via a GPIB interface. Because the signal intensity is very low (averaged peak signal around 0.15 photon per laser pulse), a photon counting technique is used to measure the dispersed fluorescence spectrum. The oscilloscope sums typically over 100 laser shots; the PC then reads this signal out and counts the number of photons present in the time interval during which the molecules pass through the field of view of the monochromator/PMT combination. At each wavelength position of the monochromator

the fluorescence intensity has been summed over 2400 laser shots to obtain the dispersed fluorescence spectrum. The frequency dependent sensitivity of the detection system is calibrated afterward in a cell experiment by the well known dispersed fluorescence spectrum of the  $A^2\Sigma^+(v'=2) \rightarrow X^2\Pi(v'')$  transition in NO,<sup>15</sup> which covers the same wavelength region as the dispersed  $a(v'=0) \rightarrow X(v'')$  fluorescence spectrum of CO. The  $A(v'=2)$  level of NO is prepared with laser radiation around 205 nm.

The spectrally broad background of the laser gives no problems in doing the dispersion measurements since the laser is kept fixed on top of an absorption line and only the resonant light is used. It gives difficulties, however, in direct absorption measurements when the laser is scanned over an absorption line: the background signal depends on the tuning of the BBO crystal, and is therefore, not constant during the scan and no correct baseline for zero absorption is obtained.

These problems are circumvented by using the molecular beam machine described above as a narrow-band detection system. The excitation laser is passed through a 1.76-m-long absorption cell, where the actual absorption experiment takes place, prior to entering the molecular beam machine. This cell is filled with a total pressure of 0–10 Torr CO at room temperature. The pressure is low enough that only the Doppler width of  $0.113 \text{ cm}^{-1}$  (FWHM) has to be taken into account, i.e., pressure broadening effects can be neglected. Only light that is transmitted through the cell and that is resonant with a transition in CO can be absorbed by CO molecules in the molecular beam on the condition that the ground state level is populated in the molecular beam. The residual Doppler width in the molecular beam is around 100 MHz due to the geometry of the machine. The nondispersed fluorescence signal, measured with a PMT in the first detection region (Fig. 1), is a direct measure for the amount of light at this specific frequency that is transmitted through the absorption cell.

By varying the pressure in the absorption cell while keeping the laser frequency on top of the molecular beam resonance, the absorption cross-section of specific transitions of the Cameron band [ $R_2(1)$ ,  $Q_2(1)$ , and  $Q_2(2)$ ] is measured (contributions of neighboring lines are in all cases below  $10^{-3}$  on top of the resonance). The fluorescence signal, corrected for laser intensity and measured as a function of pressure in the absorption cell, yields the peak absorption cross-section for all the absorption lines. The technique employed for the absorption measurements is limited to absorption lines that are isolated, and that start from levels in the electronic ground state that are sufficiently populated both in the absorption cell and in the molecular beam. Direct information is obtained, however, on exactly those levels that are relevant in molecular beam studies.

## B. Results and discussion

Figure 2 shows the dispersed fluorescence spectrum of the  $a(v'=0) \rightarrow X(v'')$  transition of CO obtained after excitation on the  $Q_2(1)$  transition, thus preparing the + parity component of the  $J=1$  level in the  $a^3\Pi_1$  state. It follows

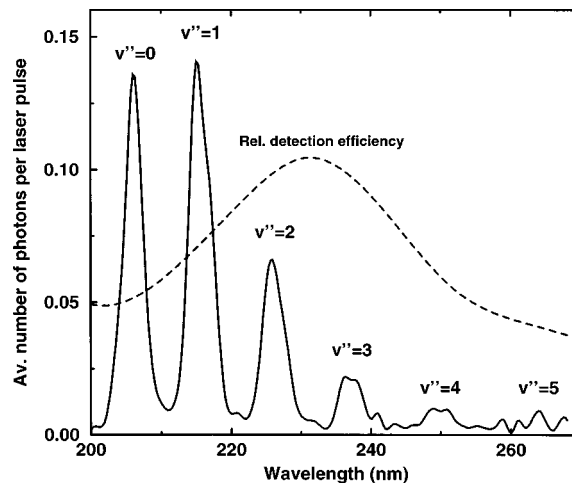


FIG. 2. Dispersed fluorescence spectrum of the spin-forbidden  $a \rightarrow X$  transition in CO. The vertical axis shows the averaged number of photons per laser pulse. The relative wavelength dependent detection efficiency of the entire detection system, indicated with the dashed curve in the figure, is calibrated using the known branching ratios of the  $\text{NO}(A \rightarrow X)$  transition, which lies in the same wavelength region. The CO dispersed fluorescence spectrum displayed in the figure is already corrected for this.

from the selection rules that the fluorescence to the different vibrational levels in the electronic ground state can only occur via  $Q_2(1)$  emission lines. Preparation of the – parity component of the same rotational level would lead to emission on  $P_2$  and  $R_2$  lines. The peaks in the dispersed fluorescence spectrum are therefore due to emission on single rotational lines. The assignment of the different vibrational levels in the electronic ground state is indicated in Fig. 2. The dispersed fluorescence spectrum displayed in Fig. 2 is already corrected for the wavelength dependent sensitivity of the detection system (indicated by the dashed line).

The height of the different peaks directly provides the relative branching ratios for the different vibrational transitions, being proportional to the Einstein  $A_{0,v''}$  coefficient. The dispersed fluorescence spectrum directly relates all  $a(v'=0) \rightarrow X(v'')$  transitions to the 0–0 transition measured in direct absorption. The resulting Einstein coefficients, with their absolute scale determined by the absorption measurements of the 0–0 transition (*vide infra*), are listed in Table I, together with the Franck-Condon factors. The measured Einstein coefficients agree rather well with the ones calculated by James.<sup>1</sup> The original values of James differ by a factor 2

TABLE I. Einstein coefficients and Franck–Condon factors derived from the dispersed fluorescence spectrum (Fig. 2), compared to the Einstein coefficients as obtained from the calculations by James (Ref. 1).

$v' \rightarrow v''$	$A_{v',v''} (\text{s}^{-1})$	F.C. factor	$A_{v',v''}^{\text{calc}} (\text{s}^{-1})$
0 → 0	97 ± 3	0.303 ± 0.010	128
0 → 1	100 ± 10	0.355 ± 0.036	136
0 → 2	47 ± 7	0.194 ± 0.029	61
0 → 3	16 ± 5	0.074 ± 0.024	16
0 → 4	7 ± 4	0.038 ± 0.022	2.5
0 → 5	6 ± 4	0.036 ± 0.024	0.22

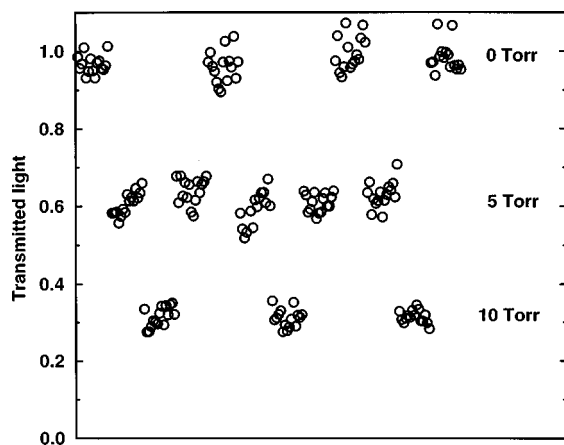


FIG. 3. Transmission through the absorption cell for three different pressures of CO and excitation on the  $Q_2(2)$  line. The first 15 data points are recorded with an evacuated cell. For the next 15 data points the cell is filled with 5 Torr of CO, after that with 10 Torr of CO, etc. The vertical axis is adjusted to a transmittance of unity for an evacuated cell.

from the ones listed here, because James considered both  $\Lambda$ -doublet components separately. The agreement between calculated and experimentally determined values for the Einstein coefficients once more validates the model as proposed by James.

The Einstein  $A$  coefficient for the 0–0 transition ( $A_{0,0}$ ) is obtained from direct absorption measurements. Figure 3 shows the results of the absorption measurements on the  $Q_2(2)$  transition. The transmitted light through the absorption cell is measured for pressures of 0, 5, and 10 Torr of CO. Each data point shows the transmitted light intensity, i.e., the intensity of the fluorescence signal in the molecular beam, for the indicated pressure, averaged over 60 laser shots. The vertical axis is adjusted to correspond to zero absorption at 0 Torr.

From these data the peak cross-section for absorption at the  $Q_2(2)$  transition is obtained. The measured data points are fitted to Beer's law:

$$I = I_0 e^{-\sigma(\nu_p)n(N'')l}, \quad (1)$$

where  $I$  is the intensity of the transmitted light,  $I_0$  the intensity of the incoming light pulse,  $\sigma(\nu_p)$  the absorption cross-section on the top of the excitation line at center frequency  $\nu_p$ ,  $l$  is the length of the absorption cell and  $n(N'')$  is the number density of molecules in the rotational level in the electronic ground state, labelled by the rotational quantum

number  $N''$ . The relative population of the various rotational levels in the ground state needed for the calculation of  $n(N'')$ , is obtained from a Boltzmann distribution for room temperature CO.

The peak absorption cross-section for the  $Q_2(2)$  line is determined from the fit. The value for the peak cross-section is indicated in Table II for all three lines of the absorption experiment. The Einstein  $A$  coefficient can be related to the peak absorption cross-section by

$$\sigma(\nu_p) = \pi r_0 f_{if} g(\nu_p), \quad (2)$$

where

$$g(\nu_p) = \frac{2\sqrt{\ln 2}}{\sqrt{\pi}\Delta\nu_D} \quad (3)$$

and

$$f_{if} = \frac{g_f}{g_i} \frac{\lambda^2}{8\pi^2 r_0 c} \frac{A_{v',v''} S_{J,N''}}{2N''+1}. \quad (4)$$

$r_0$  is the classical electron radius,  $g(\nu_p)$  the value of the normalized Doppler profile with Doppler width  $\Delta\nu_D$  (in  $\text{cm}^{-1}$ ) at the peak position of the transition and  $f_{if}$  the oscillator strength of the transition. The oscillator strength contains the degeneracy of the final ( $g_f$ ) and initial ( $g_i$ ) state ( $g_f/g_i = 2$  because of the  $\Lambda$ -doubling in the excited state), the wavelength of the  $a \leftarrow X$  transition  $\lambda$ , the normalized Hönl–London factor  $S_{J,N''}/(2N''+1)$  and the Einstein  $A$  coefficient for the given vibrational transition. The calculated Hönl–London factors<sup>1,16</sup> as well as the resulting Einstein coefficient for the transitions probed in the experiment are also found in Table II. From these data an averaged Einstein coefficient of  $A_{0,0} = 97 \pm 3 \text{ s}^{-1}$  is derived for the  $a(v' = 0) \leftarrow X(v'' = 0)$  transition.

The value of the Einstein  $A$  coefficient of the  $a(v' = 0) \rightarrow X(v'' = 0)$  transition in CO as obtained from the direct absorption measurements differs from the value that we have obtained previously from cavity ring down (CRD) absorption experiments<sup>17</sup> by a factor of 2.5. The explanation for this might be found in the fact that the CRD measurements are performed for the band-head of the  $Q_3$ -branch, which is much weaker than the transitions to the  $\Omega = 1$  ladder. An additional (weak) coupling of the  $a^3\Pi$  state to states other than the  $A^1\Pi$  state will, therefore, have a relatively large influence on the oscillator strength of transitions to levels in the  $\Omega = 2$  ladder.

TABLE II. For the excitation lines used in the experiment the rotational quantum number of the upper state  $J$ , the peak absorption cross-section  $\sigma(\nu_p)$ , the Hönl–London factor (H.L.), the Einstein coefficient  $A_{0,0}$  obtained from the peak absorption cross-section, the lifetime as determined from absorption and dispersion measurements  $\tau_{\text{abs}}$ , and the lifetime determined from the two-point measurements  $\tau_{2p}$  are given.

Exc. line	$J$	$\sigma(\nu_p) (10^{-19} \text{ cm}^2)$	H.L.	$A_{0,0} (\text{s}^{-1})$	$\tau_{\text{abs}} (\text{ms})$	$\tau_{2p} (\text{ms})$
$R_2(0)$	1		0.994		$3.67 \pm 0.20$	$3.4 \pm 0.4$
$R_2(1)$	2	$4.2 \pm 0.6$	0.482	$92 \pm 14$	$3.78 \pm 0.20$	
$Q_2(1)$	1	$4.8 \pm 0.5$	0.497	$103 \pm 11$	$3.67 \pm 0.20$	$3.8 \pm 0.5$
$Q_2(2)$	2	$4.39 \pm 0.16$	0.481	$97.1 \pm 3.5$	$3.79 \pm 0.20$	

Combining the results of the dispersion and the absorption measurements, the lifetime  $\tau(J, \Omega')$  of a certain rotational level of the  $a^3\Pi$  state labelled by the quantum numbers  $J$  and  $\Omega'$  is calculated via:<sup>1</sup>

$$\tau(J, \Omega') = [c_{\Omega', 1}^2(J) \sum_v n A_{0, v}^{-1}]^{-1}, \quad (5)$$

where  $c_{\Omega', 1}^2(J)$  represents the amount of  $\Omega=1$  character for the specific level labelled by  $J$  and  $\Omega'$ .<sup>18</sup> Since  $c_{\Omega', 1}^2(J)$  strongly depends on  $J$  and  $\Omega'$ , the lifetime of the excited state depends strongly on these parameters as well. Using this expression, the lifetime of the  $J=1$  level in the  $\Omega'=1$  ladder is determined to be  $3.67 \pm 0.20$  ms. The lifetime  $\tau_{\text{abs}}$  of the  $a^3\Pi$  levels of the different transitions used in the absorption experiment, calculated via this model, is indicated in Table II.

The combination of dispersion and direct absorption measurements provides a general tool to measure lifetimes even of very weak transitions. The absorption technique as applied here is generally applicable to obtain peak cross-sections of molecules with a well separated spectrum even with a broad-band light source.

The averaged lifetime of the  $a^3\Pi$  state that follows from our absorption and dispersion measurements,  $\tau_{\text{av}} = 11.0 \pm 0.6$  ms [corresponding to an oscillator strength of  $(1.26 \pm 0.07) \times 10^{-7}$ ], can directly be compared to a number of values reported in literature before.<sup>2,3,6,7</sup> It should be remembered that the value determined in the present experiment is derived for single, low lying, rotational levels in the  $a^3\Pi_1(v'=0)$  state, and is only afterward averaged over many rotational levels.

### III. TWO-POINT LIFETIME MEASUREMENTS

An alternative way to determine the lifetime for long lived species is to detect the fluorescence signal at two different positions, separated by a distance  $s$  (as schematically indicated by the second and third detection region in Fig. 1). The ratio of the fluorescence intensity recorded with PMTs at either position can be measured as a function of the time-delay  $\Delta t$  by varying the velocity  $v$  of the metastable species in the beam. The ratio of the two integrated PMT-signals  $I_2/I_1$  is related to the lifetime  $\tau$  of the laser prepared rotational level in the  $a^3\Pi$  state via:

$$\frac{I_2}{I_1} \propto e^{-\Delta t/\tau}. \quad (6)$$

By changing  $\Delta t$ , i.e., the carrier gas, the exponentially decaying fluorescence curve can be probed. The method relies on the fact that only the ratio of the two signals is needed to extract the lifetime.

This might not be obvious at first sight. First, both PMTs see a different solid angle and have a different detection efficiency for photons. This effect is, however, constant for all the measurements and is just a prefactor which is independent of the carrier gas. Second, upon changing the carrier gas, the velocity of the beam is changed and thereby the residence time in the two detection regions is changed. The longer the molecules spend in the detection area (i.e., the

slower they move) the more photons will be emitted in that time period, leading to an increase in fluorescence signal. Under the assumption that the time that the molecules spend in the detection region is much smaller than the radiative lifetime, this effect is proportional to  $1/v$  for both PMTs and cancels out if the ratio of both signals is considered.

Care has to be taken of the mass-focusing effect, which causes a distribution of the CO molecules perpendicular to the molecular beam axis that depends on the mass of the carrier gas.<sup>13,19</sup> The mass focusing effect can be neglected, however, if a narrow, low divergence molecular beam is used for these experiments.

Finally, alignment and polarization effects could influence the determination of the radiative lifetime. The spatial orientation of the laser polarization vector causes the molecules to radiate with a certain spatial anisotropy. It is assumed that the spatial fluorescence profile does not change when the carrier gas, and thereby the velocity of the metastable CO molecules, is changed. This is explicitly verified for the laser polarization vector both parallel and perpendicular to the molecular beam axis, by measuring the ratio of the fluorescence intensity emitted in vertical and horizontal direction as a function of the velocity of the metastable CO molecules.

### A. Experiment

For the two-point lifetime measurements the two detection regions in the UHV system (Fig. 1, detection areas 2 and 3 which are located 1 and 1.8 m downstream from the excitation region, respectively) are used. The molecules enter the UHV system through a 1.2 mm diam diaphragm, located 0.5 m downstream from the nozzle opening. In combination with the 0.8 mm diam skimmer (4 cm downstream from the nozzle opening), this diaphragm transmits a well collimated molecular beam with a low divergence to the UHV system. The base pressure in the flight tube is below  $10^{-9}$  Torr during the measurements. The (nondispersed) fluorescence of the laser prepared metastable CO molecules is detected by two different PMTs. Both PMTs are looking perpendicularly at the molecular beam in vertical direction (i.e., perpendicular to the plane of the molecular beam and the excitation laser beam).

The fluorescence signal of both PMTs is simultaneously measured, summed over typically 1000–3000 laser shots to get reasonable photon statistics, and read out by a PC. The integrated intensities of the fluorescence signals are afterward divided to obtain the desired ratio. The two-point measurements have been performed for 20% CO seeded in He, Ne, Ar, Kr, and Xe using excitation on the  $R_2(0)$  and  $Q_2(1)$  line. By varying the time-delay between the pulsed valve and the excitation laser for each carrier gas, the number of data points on the exponentially decaying curve could be increased using the velocity distribution of molecules present in the gas pulse.

### B. Results and discussion

Figure 4 shows the data points (circles with error bars) that are obtained for the different carrier gasses and time-

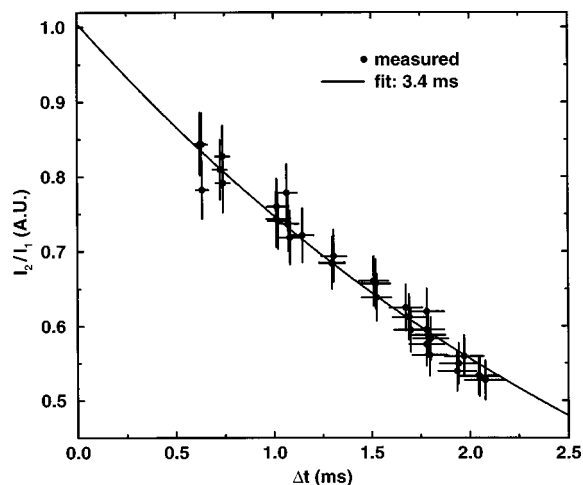


FIG. 4. The radiative lifetime of the  $J=1$  - parity level in the  $a^3\Pi_1$  state [populated via excitation on the  $R_2(0)$  transition] is recorded with the two-point measurement technique. The horizontal axis shows the time delay between the two PMT-signals. In the vertical direction the ratio of the integrated fluorescence signal (signal of second PMT divided by the signal of the first PMT) is plotted. The smooth curve shows the best fitting exponentially decaying curve, corresponding to a radiative lifetime of 3.4 ms.

delays. Laser excitation on the  $R_2(0)$  transition (populating the - parity level of the  $J=1$   $\Lambda$ -doublet in the  $a^3\Pi_1$  state) is used to obtain these data points. The horizontal axis shows the time delay  $\Delta t$  between the two PMT signals for each data point. The error bar in this direction is determined by the width of the fluorescence peaks at either position. This width (10% of the mean arrival time) is limited by the velocity distribution of the metastable CO molecules in the beam and the solid angle that the PMTs register. The smooth curve is the exponential fit, and corresponds to a lifetime of  $3.4 \pm 0.4$  ms. The last column of Table II shows the lifetime  $\tau_{2p}$  of the upper level as obtained in the two-point lifetime measurements both for excitation on the  $R_2(0)$  and the  $Q_2(1)$  absorption line.

The two-point lifetime measurement technique is a very direct way to obtain the lifetime and is generally applicable for species that have radiative lifetimes between 100  $\mu$ s and a few ms. A disadvantage of this technique is that one cannot discriminate against other nonradiative loss channels. An important loss channel in the molecular beam might be collisional redistribution. Normally collisions under these kind of circumstances are negligible, since processes that are monitored are typically on the (sub) nanosecond or microsecond time scale. In the experiment reported here the molecules fly freely during up to 2 ms. Because the lifetime of the lowest rotational levels in the  $\Omega=1$  ladder are the shortest, any collisional redistribution to other levels in the  $a^3\Pi_1$  state or quenching to the electronic ground state is an extra loss channel for fluorescence and leads to an underestimation of the lifetime. For this reason the base pressure in the flight tube used for these experiments is kept below  $10^{-9}$  Torr during the experiments, and collisions with background gas can for this reason be neglected. It has been explicitly checked that only upon increasing the base pressure up to

$10^{-6}$  Torr, collisional redistribution can be observed via a small reduction of the measured radiative lifetime.

Alternatively, it might be that collisional redistribution of metastable CO molecules within the molecular beam can no longer be neglected over such a long flight time. The relative velocity between molecules in the beam is very low, which might lead to large collisional redistribution rates. To decrease the possibility of collisions within the molecular beam, the first detection region used in these experiments is more than 3000 nozzle diameters downstream from the nozzle opening, thereby reducing the density, and thus the probability of collisions within the beam.<sup>20</sup> To check on the absence of collisional relaxation via this mechanism the lifetime measurements are performed with different backing pressures behind the pulsed valve, thereby varying the number density of molecules in the beam. It is observed that for all backing pressures up to 2 bar the measured lifetime is the same within error bars. The radiative lifetime of the  $J=1$  levels of the  $a^3\Pi_1(v=0)$  state, is therefore, determined under truly collision-free conditions.

#### IV. CONCLUSIONS

Detection of the  $a \rightarrow X$  fluorescence allowed for accurate, state-specific determination of the radiative lifetime for the lowest rotational levels in the  $\Omega=1$  component of the  $a^3\Pi$  state via two different techniques. From direct absorption measurements the Einstein coefficient for the  $a(v=0) - X(v=0)$  transition in CO is determined to be  $97 \pm 3 \text{ s}^{-1}$ . In combination with the dispersed fluorescence spectrum, the absolute values of the Einstein coefficient of the other  $a(v=0) - X(v'')$  transitions are determined as well, yielding the possibility to calculate the radiative lifetime of single rovibrational levels in the  $a^3\Pi$  state. A value of  $3.67 \pm 0.20$  ms for the  $J=1$   $\Lambda$ -doublet in the  $a^3\Pi_1(v=0)$  state was found. The two-point lifetime measurement technique gives a lifetime of  $3.4 \pm 0.4$  ms for the lower and  $3.8 \pm 0.5$  ms for the upper component of this same  $\Lambda$ -doublet. The averaged value for the radiative lifetime of the  $J=1$   $\Lambda$ -doublet obtained from these experiments is thus determined to be  $3.64 \pm 0.17$  ms.

#### ACKNOWLEDGMENTS

This work is part of the research program of the Stichting voor Fundamenteel Onderzoek der Materie (FOM), which is financially supported by the Nederlandse Organisatie voor Wetenschappelijk Onderzoek (NWO), and receives direct support by NWO via PIONIER Grant No. 030-66-89. The authors would like to thank Esther van den Berg for assisting in the experiments.

<sup>1</sup>T. C. James, J. Chem. Phys. **55**, 4118 (1971).

<sup>2</sup>V. Hasson and R. W. Nicholls, J. Phys. B **4**, 681 (1971).

<sup>3</sup>A. R. Fairbairn, J. Quant. Spectrosc. Radiat. Transf. **10**, 1321 (1970).

<sup>4</sup>T. G. Slanger and G. Black, J. Chem. Phys. **55**, 2164 (1971).

<sup>5</sup>W. L. Borst and E. C. Zipf, Phys. Rev. A. **3**, 979 (1971).

<sup>6</sup>G. M. Lawrence, Chem. Phys. Lett. **9**, 575 (1971).

<sup>7</sup>T. C. James, J. Mol. Spectrosc. **40**, 545 (1971).

- <sup>8</sup>R. T. Jongma, G. Berden, D. van der Zande, Th. Rasing, H. Zacharias, and G. Meijer, *Phys. Rev. Lett.* **78**, 1375 (1997).
- <sup>9</sup>R. T. Jongma, G. Berden, Th. Rasing, H. Zacharias, and G. Meijer, *Chem. Phys. Lett.* **273**, 147 (1997).
- <sup>10</sup>J. M. Price, A. Ludviksson, M. Nooney, M. Xu, R. M. Martin, and A. M. Wodtke, *J. Chem. Phys.* **96**, 1854 (1992).
- <sup>11</sup>M. Drabbels, C. G. Morgan, D. S. McGuire, and A. M. Wodtke, *J. Chem. Phys.* **102**, 611 (1995).
- <sup>12</sup>R. T. Jongma, G. Berden, Th. Rasing, H. Zacharias, and G. Meijer, *J. Chem. Phys.* **107**, 252 (1997).
- <sup>13</sup>R. T. Jongma, Th. Rasing, and G. Meijer, *J. Chem. Phys.* **102**, 1925 (1995).
- <sup>14</sup>R. T. Jongma, Ph.D. thesis, University of Nijmegen, The Netherlands, 1997.
- <sup>15</sup>L. G. Piper and M. Cowles, *J. Chem. Phys.* **85**, 2419 (1986).
- <sup>16</sup>R. W. Field, S. G. Tilford, R. A. Howard, and J. D. Simmons, *J. Mol. Spectrosc.* **44**, 347 (1972).
- <sup>17</sup>R. T. Jongma, M. G. H. Boogaarts, and G. Meijer, *J. Mol. Spectrosc.* **165**, 303 (1994).
- <sup>18</sup>The values  $c_{\Omega',k}$  are calculated using the model of Field *et al.* (Ref. 16) to determine the energy of rotational levels in the  $a^3\Pi$  state. In this model all the  $\Omega$ -ladders are interacting with each other. From the wavefunction belonging to the specific quantum state labelled by  $J$  and  $\Omega'$ , the amount of  $\Omega = k$ -character is calculated by squaring  $c_{\Omega',k}(J)$ .
- <sup>19</sup>*Atomic and Molecular Beam Methods, Vols. I and II*, edited by G. Scoles (Oxford University Press, New York, 1988/1992).
- <sup>20</sup>In an initial attempt to determine the lifetime via this technique, the first detection region was only 300 nozzle diameters downstream from the nozzle opening and a value of 1.1 ms was found for the  $J = 1$   $\Lambda$ -doublet of the  $a^3\Pi_1$  state (Ref. 14).